

Chapter 1

FERMI SURFACE, PSEUDOGAPS AND DYNAMICAL STRIPES IN $\text{La}_{2-x}\text{Sr}_x\text{CuO}_4$

A. Fujimori¹, A. Ino², T. Yoshida¹, T. Mizokawa¹

¹*Department of Physics and Department of Complexity Science and Engineering, University of Tokyo, Bunkyo-ku, Tokyo 113-0033, Japan*

²*Japan Atomic Energy Research Institute, SPring-8, Mikazuki, Sayo, Hyogo 679-5198, Japan*

Z.-X. Shen, C. Kim

Department of Applied Physics and Stanford Synchrotron Radiation Laboratory, Stanford University, Stanford, CA94305, U.S.A.

T. Kakeshita, H. Eisaki, S. Uchida

Department of Advanced Materials Science, University of Tokyo, Bunkyo-ku, Tokyo 113-0033, Japan

Abstract Doping dependence of the electronic structure of $\text{La}_{2-x}\text{Sr}_x\text{CuO}_4$ (LSCO) has been systematically studied in a series of photoemission measurements. The unusual spectral features in the underdoped regime are attributed to the formation of dynamical stripes and the opening of large and small pseudogaps.

1. INTRODUCTION

The most remarkable feature in the high- T_c cuprates is their characteristic phase diagram as a function of hole doping or band filling, which covers from the antiferromagnetic insulating phase near the undoped limit to the normal Fermi-liquid phase in the overdoped regime with the intervening superconducting phase. Furthermore, in the underdoped superconducting phase, “non-Fermi-liquid” properties such as pseudogap behaviors are observed.

In order to systematically understand the origin of the phase diagram and the nature of each phase, $\text{La}_{2-x}\text{Sr}_x\text{CuO}_4$ (LSCO) is a unique system in that it covers the whole range of the phase diagram in a single system. In addition, it has the simplest crystal structure with single CuO_2 layers and its hole concentration is rather accurately determined by the Sr concentration x (plus small oxygen non-stoichiometry). On the other hand, LSCO is complicated in that it undergoes a structural distortion from the high-temperature tetragonal (HTT) phase to the low-temperature orthorhombic (LTO) phase in the superconducting compositions and even has an inherent instability towards the low-temperature tetragonal (LTT) phase. The latter phase is realized in $\text{La}_{2-x-y}\text{Nd}_y\text{Sr}_x\text{CuO}_4$ (LNSCO), accompanied by the ordering of charge and spins in a stripe form, especially around $x \sim 1/8$ [1]. Transport measurements of LNSCO have shown that the static stripes are indeed one-dimensional metals [2]. Recently, LNSCO with $y = 0.4$ and $x = 0.12$ was studied by angle-resolved photoemission spectroscopy (ARPES) by Zhou *et al.* [3]. They observed Fermi surface features characteristic of a (quarter-filled) one-dimensional metal, namely, confinement of spectral weight within $|k_x|, |k_y| < \pi/4$. In LSCO, the stripes are not static but are thought to remain dynamical fluctuations, as reflected on the incommensurate inelastic neutron peaks [4].

In this article, we summarize the results of our photoemission studies on LSCO, focusing on the systematic evolution of the electronic structure as a function of hole doping including the formation of the pseudogaps. Some unusual spectral features characteristic of LSCO are indeed attributed to the dynamical stripes.

2. BAND DISPERSION AND FERMI SURFACE

The experimental band structure of optimally doped LSCO ($x \simeq 0.15$) studied by ARPES [5, 6] is similar to that of $\text{Bi}_2\text{Sr}_2\text{CaCu}_2\text{O}_8$ (BSCCO), which have been extensively studied by ARPES, as shown in Fig. 1.1. The band is flat around $\mathbf{k} = (\pi, 0)$ [especially along the $(\pi, 0)$ direction] while the band crossing the Fermi level (E_F) around $(\pi/2, \pi/2)$ is strongly dispersive. The “flat band” rises with x , crosses E_F at $x \sim 0.2$ and goes above E_F for $x > 0.2$ [6]. With decreasing x , the flat band is lowered, and around $x \sim 0.1$ it becomes as low as ~ 0.1 eV below E_F [7].

As the position of the flat band relative to E_F changes with x , the Fermi surface topology changes. For $x > 0.2$, Fermi surface crossing occurs on the $(0, 0) - (\pi, 0)$ line, giving rise to an electron-like Fermi surface

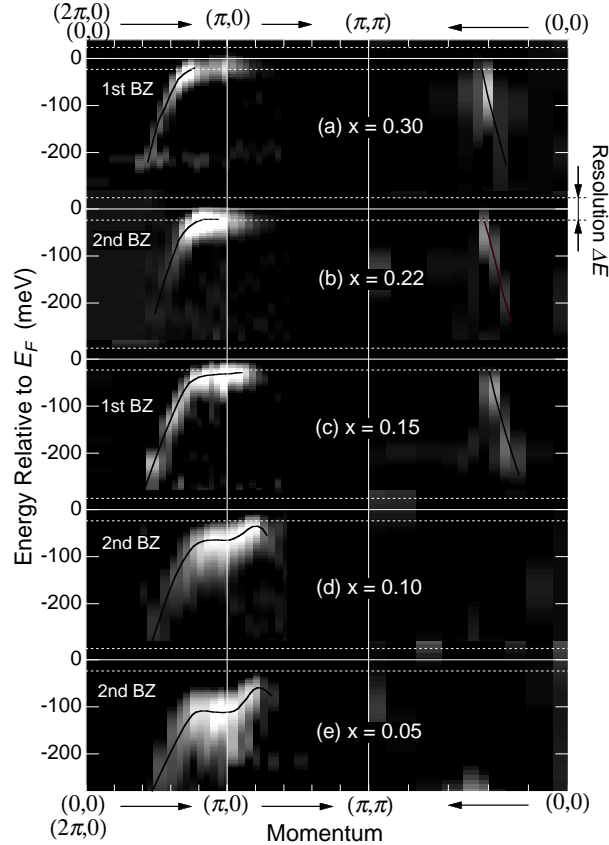


Figure 1.1 Band dispersions in LSCO [6].

centered at $(0, 0)$ [5], as shown in Fig. 1.2. For $x < 0.2$, Fermi-surface crossing occurs on the $(\pi, 0) - (\pi, \pi)$ line, resulting in a hole-like Fermi surface centered at (π, π) as in the other cuprates, as shown in the same figure. Real Fermi-surface crossing does not occur at the measurement temperatures (~ 10 K) for most of the samples, however, because a superconducting gap or a pseudogap is opened on the underlying ‘‘Fermi surface’’. In such a case, the Fermi surface can only be defined by a minimum gap locus [8]. As for the dispersive band around $(\pi/2, \pi/2)$, the doping dependent shift is small. The doping dependence of the shift is strong for the band around $(\pi, 0)$ and weak for the band around $(\pi/2, \pi/2)$, as in the case for BSCCO [9].

Figure 1.2 also shows that, for the underdoped samples, the ‘‘Fermi surface’’ around $(\pi, 0)$ become rather straight. This suggests that a one-dimension-like electronic structure is realized, giving support to the

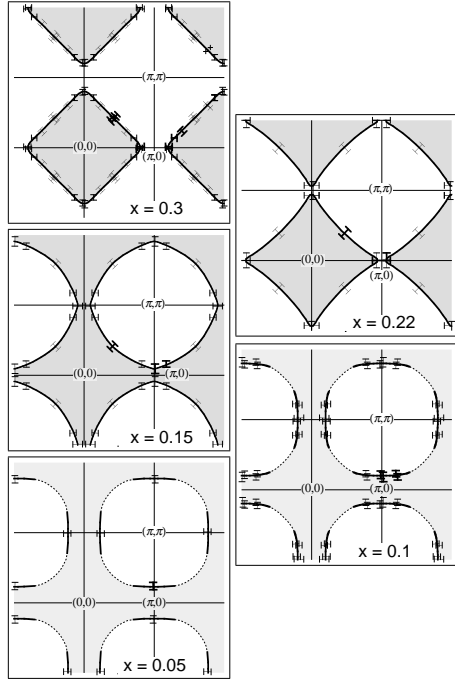


Figure 1.2 Fermi surface or minimum gap locus of LSCO determined by band dispersions in the ARPES spectra [6].

formation of dynamical stripes. Very recently, the evolution of the Fermi surface described above was demonstrated in terms of two-dimensional intensity plots [10], too, as had been made for LNSCO [3]. Here, it should be noted that the spectral weight distribution around $(\pi, 0)$ is rather complicated, making the determination of the Fermi surface nontrivial. In addition to the intrinsic broadness of spectral features and the opening of the superconducting gap and pseudogap around $(\pi, 0)$, spectral weight remains finite at E_F around $(\pi, 0)$ even for $x = 0.3$, where the band is thought to be located well above E_F .

The intensity of the dispersive band around $(\pi/2, \pi/2)$ is unusually low in LSCO. In the underdoped samples ($x < 0.15$), most of its spectral weight is transferred to the higher binding energies of ~ 0.5 eV, where the insulating samples ($x \sim 0$) show the lower Hubbard band, as shown in Fig. 1.3 [6, 7]. Here, the insulating sample $x = 0.03$ shows essentially the same band dispersion as the parent Mott insulator such as $\text{Sr}_2\text{CuO}_2\text{Cl}_2$ [11]. The disappearance of the $(\pi/2, \pi/2)$ band or the “nodal” quasi-particle (QP) band can be intuitively understood as due to the presence of dynamical stripes, which extend along the vertical $(0, \pi)$ or horizontal

$(\pi, 0)$ direction. That is, the propagation of QP along the diagonal direction would be always disturbed by the hole-poor region of the stripe phase, whereas the propagation along the Cu-O bond direction would be disturbed only with the probability of 50 %. In contrast to the nodal QP, the flat band around $(\pi, 0)$ is robust against the decrease of hole concentration. It persists down to $x \sim 0.05$, i.e., down to the superconductor-insulator boundary, and then spectral weight transfer to the lower Hubbard band at ~ 0.5 eV below E_F occurs.

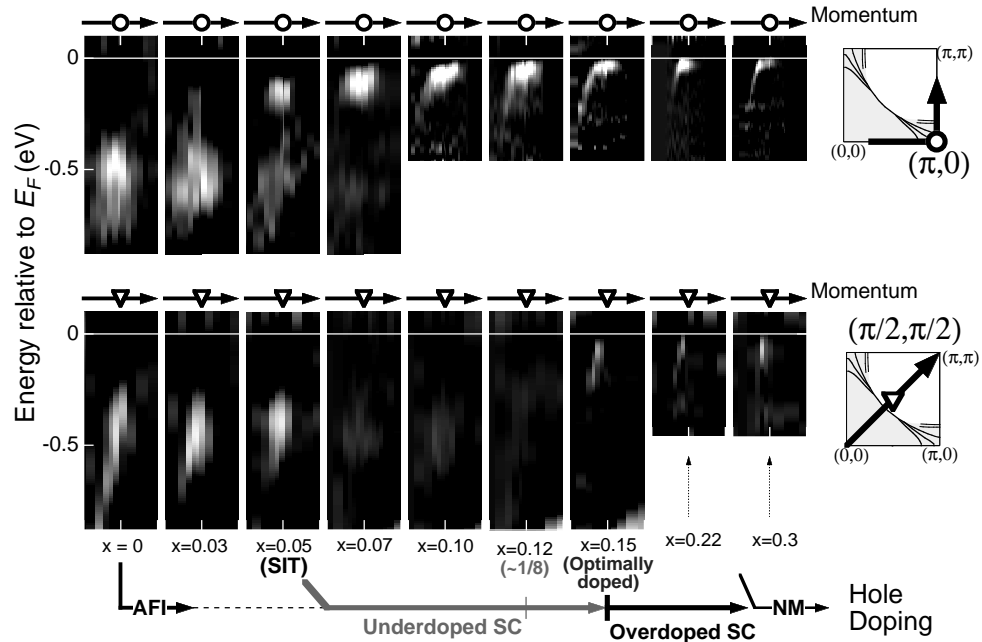


Figure 1.3 Doping dependence of the band dispersions near $(\pi, 0)$ and $(\pi/2, \pi/2)$ in LSCO [6].

2.1. CHEMICAL POTENTIAL SHIFT

According to the stripe picture, the hole density along each stripe is constant (0.5 per Cu-Cu distance, namely, each stripe is quarter-filled) whereas the density of the charge stripes changes with hole doping. Therefore, as long as the separation between the stripes is sufficiently large so that the inter-stripe interaction is negligible, the energy of the system per hole remains almost constant. This means that the chemical potential of electron or hole remains unchanged with hole doping and

hence apparently remains fixed. The pinning of the chemical potential has indeed been observed in LSCO for $x < 0.12$ [12].

Figure 1.3 demonstrates that ARPES data show remarkable changes around $x = 0.05$ [7]. The spectral change at $x \sim 0.05$ may reflect the superconductor-to-insulator transition at this composition or the change from the dynamical to static stripes because the coherent spectral weight near E_F , which remains appreciable around $(\pi, 0)$, disappears below this x . This may also reflect the change from the vertical to diagonal stripes at $x < 0.05$ as observed by a recent neutron scattering study [13] because the hole motion along the Cu-O bond direction would be hindered in this composition range. In the narrow composition range around $x = 0.05$, the spectrum at every \mathbf{k} is modeled as a superposition of that of the insulator ($x \sim 0$) and that of the superconductor ($x \simeq 0.07$).

3. LARGE PSEUDOGAP

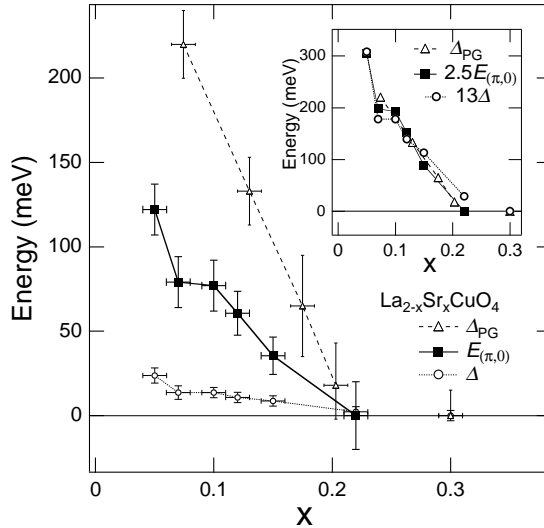


Figure 1.4 Magnitudes of the superconducting gap Δ , large pseudogap Δ_{PG} and the energy position of the $(\pi, 0)$ flat band $E_{(\pi,0)}$ as functions of hole doping x [6].

Angle-integrated photoemission (AIPES) studies of LSCO has revealed a reduction of the density of states (DOS) at E_F and around it below $x \sim 0.2$ [14]. This reduction tracks the decrease of the electronic specific heat [15, 16] and that of the Pauli component in the uniform magnetic susceptibility [18] with decreasing x , which occurs in the same composition range. These phenomena are consistent with the Fermi-surface crossing of the flat band at $x \simeq 0.2$ since the flat band is

expected to naturally give a high DOS. The downward shift of the flat band away from E_F with decreasing x reduces the DOS at E_F . If we call the energy region around E_F with the reduced DOS a “large pseudogap”, the large pseudogap expands from zero at $x \sim 0.2$ to ~ 0.1 eV at $x \sim 0.1$. As the magnitude Δ_{PG} of the large pseudogap increases with decreasing x (Fig. 1.4), the temperature $T_{\chi_{\max}}$ at which the magnetic susceptibility takes the maximum increases [18], so that the relationship $\Delta_{PG}/k_B T_{\chi_{\max}} \sim 3$ holds.

The appearance of a pseudogap below $x = 0.2$ and its nearly linear increase with decreasing hole concentration has been identified in recent specific heat measurements [17]. This observation together with the fact that Δ_{PG} is of the order of the in-plane super-exchange coupling constant J suggest that the antiferromagnetic coupling between the Cu spins is responsible for the formation of the large pseudogap. Such a scenario is consistent with the $t - J$ model calculation of photoemission spectra by Jaklič and Prelovšek [19].

4. SMALL PSEUDOGAP AND SUPERCONDUCTING GAP

In addition to the large pseudogap, AIPES [14, 20] and ARPES [10] studies have revealed that a superconducting gap of several meV is opened at E_F . The gap is identified as a leading edge shift or a dip in the symmetrized spectra on the Fermi surface, $A(k_F, \omega) + A(k_F, -\omega)$. The magnitude of the gap reaches the maximum near $(\pi, 0)$ and satisfies the BCS relationship of a d -wave superconductor $2\Delta/k_B T_C \sim 4$ in the optimally-doped samples whereas $2\Delta/k_B T_C \gg 4$ in the underdoped samples. It is found that Δ increases with decreasing x and that Δ_{PG}/Δ remains roughly constant in the underdoped regime (Fig. 1.4), implying a correlation between the large pseudogap and the superconducting gap, and hence a close connection between the antiferromagnetic correlations and the superconductivity. Although our measurements were made largely in the superconducting state, we expect that the superconducting gap of the underdoped samples, which is much larger than $4k_B T_C$, would not collapse above T_C and remains as a normal-state gap or a “small pseudogap” as in BSCCO [21].

5. EVOLUTION OF ELECTRONIC STRUCTURE WITH HOLE CONCENTRATION

The photoemission results described have revealed the following characteristic hole concentration regions in LSCO:

- (i) $x > 0.2$: Normal Fermi-liquid regime with an electron-like Fermi surface. The effective mass is enhanced with decreasing x . The flat band is located above E_F . The Wilson ratio approaches 2 in the heavily overdoped limit [18], indicating that the system is a strongly correlated two-dimensional Fermi liquid. The T_c becomes the highest in this crossover regime.
- (ii) $0.12 < x < 0.2$: Crossover regime between the normal Fermi liquid and the dynamical stripe phase. The flat band is lowered below E_F and the Fermi surface becomes hole-like. The QP is weakened around the nodal point because of the stripe fluctuations. The pseudogaps start to form.
- (iii) $0.05 < x < 0.12$: Metallic (superconducting) phase with dynamical stripes. The Fermi surface becomes straight lines around $(\pi, 0)$, implying one-dimensional character, and the nodal QP loses most of its spectral weight. The chemical potential is pinned associated with the stripe formation. The large pseudogaps are fully developed. The Wilson ratio becomes ~ 1 [18], suggesting that the spectral weight of low-energy fluctuations are depleted due to the opening of the large pseudogap.
- (iv) $x < 0.05$: Insulating state with segregated holes.

One may ask the question of how the stripes and the pseudogaps are related with each other in the underdoped regime. Presumably, the hole-poor part of the stripe phase is more insulator-like and contributes to the gap-like DOS and hence to the large pseudogap. The hole-rich part contributes to the finite DOS at E_F and to the superconducting gap (and the small pseudogap).

Finally, let us come back to the question of whether the antiferromagnetic correlation helps the superconductivity or competes with it. The similar doping dependence of the large pseudogap and the superconducting gap may suggest that the antiferromagnetic correlation, which is likely to be the origin of the large pseudogap, is responsible for the Cooper pairing. On the other hand, if the antiferromagnetic correlation is the origin of the large pseudogap, it follows that the antiferromagnetic correlation disrupts the superconductivity through the reduction of the DOS at E_F . Then the antiferromagnetic correlation helps and disrupts the superconductivity simultaneously. This is analogous to the situation of phonon-mediated superconductivity in which too strong electron-phonon interaction causes lattice instability and thus disrupts the superconductivity. Now, it is illuminating to plot the phase diagram of LSCO against the chemical potential μ instead of hole concentration x , as shown in Fig. 1.5. Since the chemical potential does not move for $0 < x < 0.12$, in the $\mu - T$ phase diagram, the underdoped region

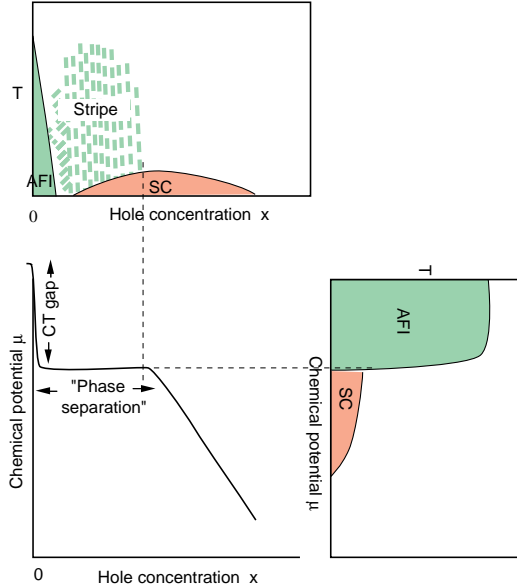


Figure 1.5 Phase diagram of LSCO plotted against the chemical potential μ [22].

collapses into a phase boundary line between the superconducting phase and the antiferromagnetic insulating phase. As the chemical potential approaches that of the parent insulator, the T_c monotonously increases due to the increased pairing potential, but eventually the superconducting state becomes unstable and is taken over by the antiferromagnetic insulating phase via a first-order phase transition. Such an instability would be inherent in strong coupling superconductors of magnetic origin [22]. Also, such a phase diagram implies the degeneracy of the antiferromagnetic and superconducting phases at the phase boundary, the situation to which SO(5) theory may be applicable [23].

Acknowledgments

We would like to thank K. Kishio, T. Kimura and K. Tamasaku for collaboration in the early stage of this work. This work is supported by a Grant-in-Aid for Scientific Research from the Ministry of Education, Science, Sports and Culture of Japan, the New Energy and Industrial Technology Development Organization (NEDO), the U. S. DOE's Office of Basic Energy Science, Division of Material Sciences. Experiments were performed at the Stanford Synchrotron Radiation Laboratory, which is operated by the Office's Division of Chemical Sciences.

References

- [1] J. M. Tranquada *et al.*, *Nature* **375**, 561 (1995).
- [2] T. Noda, H. Eisaki and S. Uchida, *Science* **286**, 265 (1999).
- [3] X. J. Zhou *et al.*, *Science* **286**, 268 (1999).
- [4] K. Yamada *et al.*, *Phys. Rev. B* **57**, 6165 (1998).
- [5] A. Ino *et al.*, *J. Phys. Soc. Jpn.* **68**, 1496 (1999).
- [6] A. Ino *et al.*, [cond-mat/0005370](http://arxiv.org/abs/cond-mat/0005370).
- [7] A. Ino *et al.*, *Phys. Rev. B* **62**, 4137 (2000).
- [8] H. Ding *et al.*, *Phys. Rev. Lett.* **78**, 2628 (1997).
- [9] D. S. Marshall *et al.*, *Phys. Rev. Lett.* **76**, 4841 (1996).
- [10] T. Yoshida *et al.*, unpublished.
- [11] B. O. Wells *et al.*, *Phys. Rev. Lett.* **74**, 964 (1995).
- [12] A. Ino *et al.*, *Phys. Rev. Lett.* **79**, 2101 (1997).
- [13] S. Wakimoto *et al.*, *Phys. Rev. B* **62**, 3547 (2000).
- [14] A. Ino *et al.*, *Phys. Rev. Lett.* **81**, 2124 (1998).
- [15] J. W. Loram *et al.*, *Physica C* **162**, 498 (1989).
- [16] N. Momono *et al.*, *Physica C* **233**, 395 (1994).
- [17] J. W. Loram *et al.*, *Physica C*, in press.
- [18] T. Nakano *et al.*, *Phys. Rev. B* **49**, 16000 (1994).
- [19] J. Jaklič and P. Prelovšek, *Phys. Rev. B* **60**, 40 (1999).
- [20] T. Sato *et al.*, *Phys. Rev. Lett.* **83**, 2254 (1999).
- [21] A. G. Loeser *et al.*, *Science* **273**, 325 (1996).
- [22] S. Tesanović, private communication.
- [23] S-C. Zhang, *Science* **275**, 1089 (1997).